J. Membrane Biol. 66, 159–169 (1982)

The Journal of
Membrane Biology

Sodium Currents in the Giant Axon of the Crab *Carcinus maenas*

M. Emilia Quinta-Ferreira, N. Arispe,* and E. Rojas

Department of Biophysics, School of Biological Sciences, University of East Anglia, Norwich NR4 7TJ, England

Summary. Measurements were made of the kinetics and steady-state properties of the sodium conductance changes in the giant axon of the crab *Carcinus maenas*. The conductance measurements were made in the presence of small concentrations of tetrodotoxin and as much electrical compensation as possible in order to minimize errors caused by the series resistance. After an initial delay of 10–150 μsec, the conductance increase during depolarizing voltage clamp pulses followed the Hodgkin-Huxley kinetics. Values of the time constant for the activation of the sodium conductance lay on a bell-shaped curve with a maximum under 180 μsec at −40 mV (at 18 °C). Values of the time constant for the inactivation of the sodium conductance were also fitted using a bell-shaped curve with a maximum under 7 msec at −70 mV. The effects of membrane potential on the fraction of Na channels available for activation studied using double pulse protocols suggest that hyperpolarizing potentials more negative than −100 mV lock a fraction of the Na channels in a closed conformation.

Key words giant axon · sodium channel · voltage clamp · crustacean nerve · Na channel gating · sodium conductance

Introduction

Titration of membrane sites by the molecules of tetrodotoxin (TTX) needed to block the action potential in nerves is often taken as evidence for a discrete distribution of sodium channels. Thus the density of these elementary units of conductance on lobster (Moore, Narahashi & Shaw, 1967) and on lobster, crab and rabbit nerve membranes (Keynes, Ritchie & Rojas, 1971) has been estimated from the amount of TTX or saxitoxin (STX) that is taken up by the nerve at the time when the block of the action potential occurs. The concentration of TTX required to halve the amplitude of the action potential in crab nerves was about 14 nM (Keynes et al., 1971).

If γ_{Na} is the conductance of a single Na channel and A is the density of Na channels, then the membrane conductance per unit area is $g_{Na}=A\gamma_{Na}$. In order to calculate γ_{Na}, A must be estimated and g_{Na} must be measured in the same preparation. Owing to the small diameter of the fibers, only a few voltage-clamp experiments on fibers from crab nerves (in which the amount of TTX taken up by the whole nerve was measured) have been attempted (Connor, 1975; Connor, Walter & McKown, 1977). These authors used the sucrose gap technique to measure and control the membrane potential in 50- to 90-μm giant axons from *Callinectes sapidus* and larger fibers from *Cancer magister*.

The purpose of this paper is to present the results obtained with a different method, namely, the double Vaseline seals technique, designed to set the voltage across the axolemma of a crab giant axon (30 to 40 μm in diameter) at a controlled value. The feedback amplifier used was provided with a positive feedback arrangement to compensate the applied voltages for the voltage drop across the resistance in series with the axolemma. The sodium current records obtained have been analyzed using the Hodgkin-Huxley (1952*b*) formalism.

A preliminary report of this work has been presented elsewhere (Arispe, Quinta-Ferreira & Rojas, 1979).

Materials and Methods

Nerve Preparation

Experiments were performed on giant axons from the meropodite section of walking legs of *Carcinus maenas*. Single nerve fibers were dissected from the main nerve bundle.

The chamber, shown diagrammatically in Fig. 1, was designed by Nonner (1969). Two petroleum jelly seals (from now on referred to as Vaseline seals) 90 μm in diameter, one over the ridges of the partitions between the pools of the chamber, and the other on top, were used. The nerve fiber was mounted at right angles between the seals. The width of the gap between the Vaseline seals on either side of pool *A* was adjusted to about the diameter of the fiber. The width of the gap in pool *B* was

* *Permanent address:* Escuela de Biologia, Universidad Central de Venezuela, Caracas.

0022-2631/82/0066-0159 $02.20

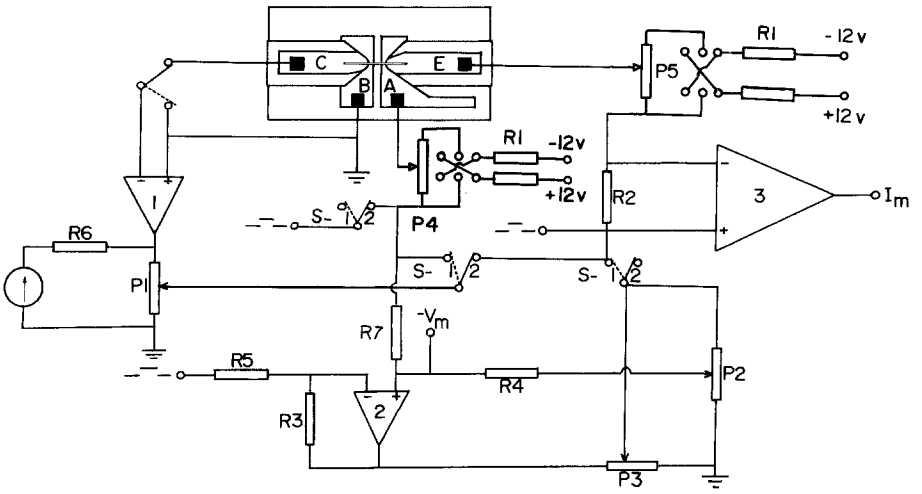

Fig. 1. Nerve chamber, electrode arrangement and feedback amplifier. The upper part represents a diagram of the chamber with a nerve fiber which extends from pool *C* to pool *E*. Four Ag/AgCl/Pt electrodes electrically connect the pools in the nerve chamber through agar bridges to the feedback amplifier. The lower part represents a diagram of the feedback amplifier. The switch *S* determines the configuration: 1 is in the Dodge-Frankenhaeuser (1958) mode and 2 is in the Nonner (1969) mode. Amplifier 1 was made of discrete components (Medica, Saarbrücken, West Germany).

$P4=P5=10^3\,\Omega$, $P1=P2=P3=10^4\,\Omega$, $R1=10^5\,\Omega$,

$R3=10^6\,\Omega$, $R5=R4=10^4\,\Omega$, $R2=10^3\,\Omega$, $R6=10^5\,\Omega$, $R7=2\times10^4\,\Omega$.

In the Nonner mode, pulses were applied directly to electrode in pool *A*. In the Dodge-Frankenhaeuser mode to the negative input of amplifier 2 (Burr-Brown 3551) through *R*5 in the voltage clamp configuration and directly to electrode in pool *E* in the current clamp mode. Amplifier 3 was a Tektronik 2A72 amplifier with an active filter. *P*4 was used to provide a holding potential and *P*5 a holding current.

adjusted between 50 and 100 μm. Pools *B* and *C* were separated by two double Vaseline seals in such a way that 200 μm length of the axon was surrounded by petroleum jelly.

Two forceps mounted on a micromanipulator were used to hold a segment of the axon (1.5 cm in length) at right angles over the partition between the pools. During these operations, the fiber was immersed in Na^+ and K^+-free artificial sea water (hereafter referred to as Na, K-free ASW). After placing the Vaseline seals, the excess solution flooding the pools was removed and the solution in pools *C* and *E* was replaced by a caesium fluoride solution. The ends of the fiber were cut in this solution. The length of the distal end (from cut end in pool *E* until the edge of the Vaseline seal facing pool *A*) was kept shorter than 500 μm.

Feedback Amplifier

The configuration of the feedback amplifier used is shown in Fig. 1 and was similar to that used to voltage clamp frog skeletal muscle fibers (Frankenhaeuser, Lindley & Smith, 1966). With the switch *S* in the diagram in position 2 the amplifier 2 was placed out of the feedback and the configuration was as described by Nonner (1969). With the switch in position 1 the configuration was as described by Hille and Campbell (1976). Electronic compensation for the voltage error along the resistance in series with the axolemma, caused by radial current flow, was used. The maximum correction amounted to $R_s=4.0\,\Omega\text{cm}^2$. The current injected by the feedback amplifier was measured either as a voltage drop across 1000 Ω resistance in series with the electrode *E* (Hille & Campbell, 1976) or as the voltage in electrode *E* divided by the resistance of the distal end of the axoplasm (Dodge & Frankenhaeuser, 1958). In general, there was reasonable agreement between these two measurements. Taking the specific resistance of the axoplasm as 35 Ωcm (Cole & Hodgkin, 1939), values of the calculated resistance ranged between 5×10^3 and $200\times10^3\,\Omega$.

Holding Potential

To determine the absolute value of the holding potential two procedures were employed. In the first procedure the position of the $h_\infty-V_1$ curve (*see* Results) was first determined. As the resting potential determined with microelectrodes is −70 mV in these fibers, h_∞ was taken as 0.7 in resting conditions. The value of the holding potential was easily calculated knowing the size of the prepulse from holding potential which gave $h_\infty=0.7$. In the second procedure only the reversal potential for I_{Na} was measured. It was necessary to obtain first an average value of the permeability ratio α $(=P_{Cs^+}/P_{Na^+})$ in fibers in which a $h_\infty-V_1$ run was also available.

The permeability ratio of Cs^+ to Na^+ ions flowing through the Na^+ channel was estimated using the Goldman-Hodgkin-Katz equation (Goldman, 1943; Hodgkin & Katz, 1949):

$$E_{Na}=\frac{RT}{ZF}\ln\frac{|Na^+|_o}{|Na|_i+\alpha|Cs^+|_i}$$

where the E_{Na} is the absolute reversal potential for I_{Na} and the other parameters have their usual meaning. With solutions CsF-2 in pools *C* and *E* and with K-free ASW in pool *A* the average of three determinations was $P_{Cs}/P_{Na}=0.007$ (*see* Fig. 3).

Data Acquisition

A digital computer (System 90, Computer Instrumentation Limited) was used on-line during the experiments. The computer was

Table 1. Composition of solutions

A. Internal solutions (pools *C* and *E*)

Name	$\|TEA^+\|$	$\|K^+\|$	$\|Na^+\|$	$\|Cs^+\|$	$\|TRIS^+\|$	Osmotic pressure (mOsm)
			(mM)			
KF-1	–	500	–	–	50	970
KF-2	–	500	47	–	10	990
CsF-1	–	–	–	500	50	950
CsF-2	–	–	47	500	10	960
CsF-3	50	–	47	500	28	918

B. External solutions (pools *A* and *B*)

Name	$\|K^+\|$	$\|Na^+\|$	$\|Mg^{2+}\|$	$\|Ca^{2+}\|$	$\|TRIS^+\|$	$\|TMA^+\|$	Osmotic pressure (mOsm)
				(mM)			
ASW	11	470	14	12	5	–	1030
K-free ASW	–	470	14	12	5	–	930
Na,K-free ASW_1	–	–	14	12	475	–	902
Na,K-free ASW_2	–	–	50	20	440	–	972
Na,K-free ASW_3	–	–	14	12	5	450	1068
Na,K-free ASW_4	–	–	50	10	440	–	966

Osmotic pressure measured with vapor pressure osmometer (Wescor, Inc. model 5100 C). The pH of all solutions was adjusted at room temperature to 7.3 ± 0.1.

used to generate a holding voltage level V_h, to generate voltage pulses V_P and to measure the voltage across the 1000 Ω resistance between the output of the feedback amplifier and electrode *E*. Each record was stored into digital magnetic tape in unformatted mode, as described elsewhere (Pynsent & Rojas, 1979). This method enabled us to store records consisting of 3072 samples in 500 msec.

The experimental protocol and data acquisition were organized using Fortran IV programs executed by the computer. The use of multiple-level buffering and two direct memory access channels enables the analog-to-digital converter (ADC) and digital-to-analog converter (DAC) to run synchronously at 10^6 Hz. This sampling rate was used to digitize the first 100 μsec of the transients to measure the capacity of the membrane in pool *A* and, assuming 1 μF/cm², to estimate the membrane area.

Data Analysis

The same computer was used after the experiments for the off-line analysis of the records. Before starting the analysis of each record, they were treated as follows:

(1) The holding current before the test and control pulses (base line) was evaluated.

(2) The test pulse and control pulse current transients (after proper scaling of the control pulse transient) were summed.

(3) Several pairs of records were averaged.

(4) The 3072 points in each averaged record were condensed into 256 values by averaging again each subsequent 12 points.

Solutions

The composition of the solutions used is given in Table 1.

Results

Ionic Currents under Voltage-Clamp Conditions

Figure 2 shows a set of 12 superimposed membrane current records from a giant axon.

To achieve good control of the membrane potential in pool *A*, the length of the fiber in that pool has to be kept below 50 μm. Under these conditions both feedback amplifier systems used in this work give very similar records, with very small leakage currents ($g_L \simeq 0.3$ mmho/cm²).

Each current record can be analyzed into three time and membrane potential-dependent components, namely, one inward and two outward components. These records are comparable to those made by Connor (1975) using the double sucrose gap technique.

The outward components can be blocked by internal application of caesium, sodium, tetraethylammonium (TEA) and 4-amino piridine (4 AP) (*see following paper*). The inward component is not affected by any of these treatments.

Tetrodotoxin (TTX) at a concentration of 5 nM reversibly blocks the inward component to half of its size before the application of TTX. Replacement of sodium by tetramethylammonium (TMA) abolishes the inward component.

This paper represents the analysis of the kinetic and steady-state properties of the early transient

current, seen in Fig. 2 which is certainly carried by sodium ions.

The following paper deals with the kinetic and steady-state characteristics of the two components of the outward currents which are carried by potassium ions.

Kinetic Characteristics of the Sodium Currents

If the ends of the fiber in pools C and E are cut in a caesium fluoride solution, the outward components of the currents seen in Fig. 2 disappear from the records. This is illustrated in Fig. 3. When the holding potential is set at a very negative value (less than -80 mV) the currents are well described by the equation

$$I_{Na} = \begin{cases} 0, & 0 \leqq t < \delta t \\ I_{Na,max}(1-\exp(-t/\tau_m))^3 \exp(-t/\tau_h), & t \geqq \delta t \end{cases} \quad (1)$$

The analysis of the currents presented in Fig. 3 suggested that it is possible to modify the Hodgkin-Huxley equations to describe the kinetic properties of the Na system in these fibers. The rest of this work deals with this analysis.

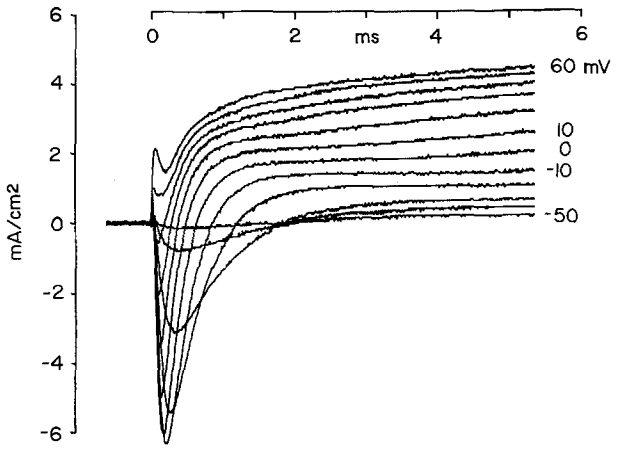

Fig. 2. Membrane currents recorded using the two amplifiers in the feedback loop. Experiment 790209: Width of A pool = 50 µm perfused with ASW at 14 °C. Solution in pools C and E: KF-1. Absolute membrane potential during some of the pulses is indicated near the current records (mV). Sampling interval 1 µsec. Reversal potential for the inward currents near 45 mV

Steady-State and Kinetic Properties of the Sodium Conductance Inactivation

Information on the effects of membrane potential on the sodium conductance inactivation was obtained from three different experimental protocols illustrated in Figs. 4, 5 and 6.

In double-pulse experiments designed to measure the steady-state values of the inactivation parameter h, the duration of the prepulse V_1 was set at 25 msec. Figure 4 summarizes the results of a double-pulse experiment of this type. The abscissa represents the membrane potential during V_1. The vertical axis was calculated as $I_{Na,max}(V_2, V_1)/I_{Na,max}(V_2, V_1 = V_h)$ where V_2 represents the potential during the test pulse and V_h the holding potential. Shown in the upper part of this Figure are the superimposed $I_{Na}(V_2, V_1)$ records. The dotted line in Fig. 4 represents the best fit of the points calculated using the empirical equation given in the legend to Table 2.

Although $h_\infty - V_1$ curves were measured in all the experiments reported here, the results from five experiments in which 5 to 25 nM TTX was used to

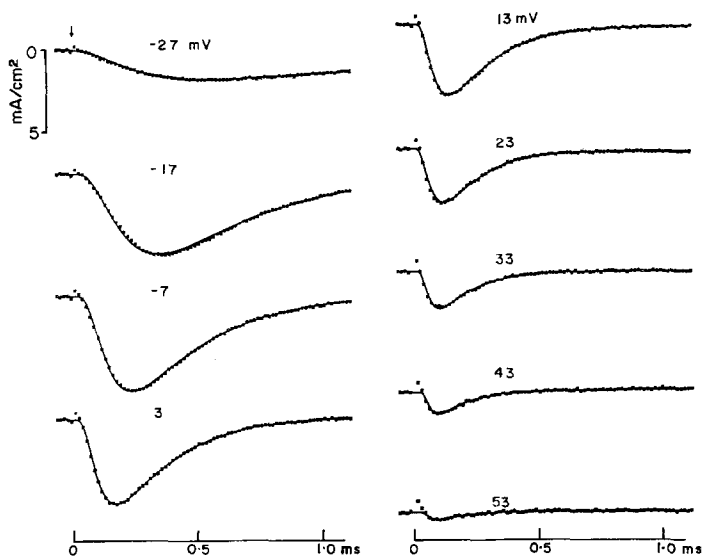

Fig. 3. Time course of the Na currents at different membrane potentials. Experiment 790508 B: Cut ends in CsF-3 at pH = 7.4. Feedback amplifier was of the Dodge-Frankenhaeuser type. Holding potential set at -87 mV. Reversal potential near 55 mV. $P_{Cs^+}/P_{Na^+} = 0.007$ (*see* Materials and Methods). Temperature 18.1 °C. Sampling interval equals 1 µsec. Interval between points equals 15 µsec. Solid lines represent the best fit to the points calculated using Eq. (1)

reduce I_{Na} and therefore to minimize the effects of the series resistance are presented in Table 2.

Assuming that $h_\infty = 0.7$ at $V_1 = -70$ mV, the steepness of the $h_\infty - V$ curve can be evaluated from the average values of the parameters A and B in Table 2. At $V_1 = -70$ mV a 16.9 mV change in potential induces an e-fold change in h_∞. This value compares rather well with the value measured in the giant axon of squid, namely, 18.0 mV at resting potential (Fig. 5 in Hodgkin & Huxley, 1952*a*). Furthermore, when h_∞ tends to 0, an e-fold change in h_∞ is obtained with 5.1 mV change in V_1.

The time constant of inactivation τ_h for membrane potentials greater than -54 mV was calculated from the least-squares fit of a single exponential function to the declining phase of the Na^+ conductance curves as presented in the next section. For potentials too small to induce a measurable I_{Na}, the double-pulse protocol was used as illustrated in Fig. 5. The duration of V_1 was augmented from 0.1 to 25 msec. It may be seen that, to a first approximation, the time course of the development of inactivation can be described as a first-order process.

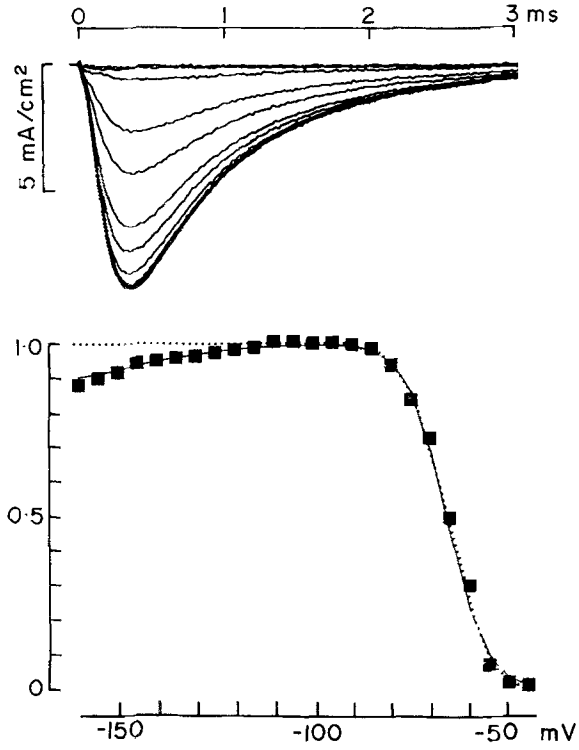

Fig. 4. Steady-state sodium conductance inactivation. Experiment 800320A: Temperature 12.6 °C. *Upper part:* 15 superimposed sodium current records obtained with a test pulse V_2 to -20 mV preceded by prepulses to the potential indicated in the abscissa of the graph (*lower part*). *Lower part:*

$$\frac{I_{Na,max}(V_2, V_1)}{I_{Na,max}(V_2, V_1 = V_h)}$$

as a function of membrane potential during the prepulse V_1. Dotted curve was calculated with equation in Table 2. Solid curve with

$$h_\infty = \left(\frac{1}{1+\exp(A+BV_1)}\right)\left(\frac{1-E}{1+\exp(C+DV_1)}+E\right)$$

and represents the least-squares best fit with $A = 13.2$, $B = 0.2$, $C = -9.11$, $D = 0.062$ and $E = 0.85$

Table 2. Steady-state parameters from $h_\infty - V_1$ curves

Experiment	A	B (mV^{-1})	V_h (mV)	Temp (°C)
800320A	13.2	0.200	−120	12.6
800320B	15.4	0.232	−105	12.6
800416	9.9	0.152	−105	14.6
800419A	13.8	0.208	−125	15.5
800419B	11.9	0.193	−125	15.5
AVE±	12.8	0.197		
SD	2.1	0.029		

Data from fitting the $h_\infty - V_1$ curve using the empirical equation $h_\infty \frac{1}{1+\exp(A+B\,V_1)}$

where V_1 is the potential during the prepulse. Thus,

$$\frac{d \ln h_\infty}{dV_1} = -B(1-h_\infty).$$

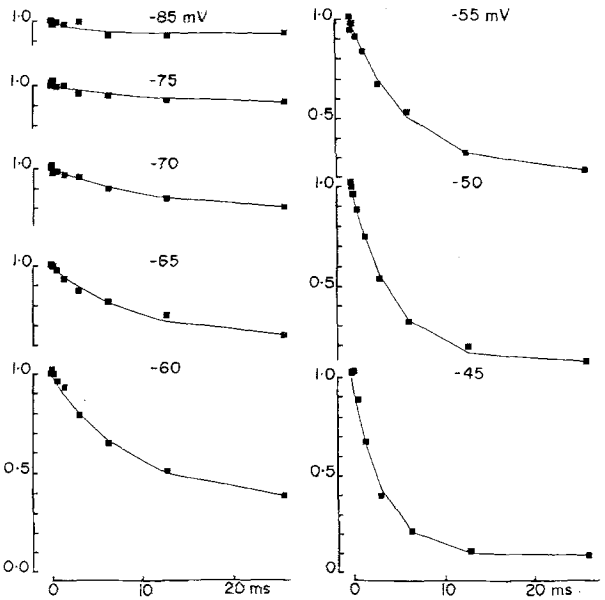

Fig. 5. Time course of the development of the fast sodium conductance inactivation. Experiment 800416: Fiber in K-free ASW plus 10 nM TTX. Cut ends in solution CsF-2. Holding potential -105 mV. Temperature 14.6 °C. Membrane potential values during the prepulse V_1 are indicated for each series of prepulse durations. Solid lines represent the least-squares fit of an exponential time function to the points. Membrane potential during test pulse -10 mV

Table 3. Kinetic and steady-state parameters for the sodium conductance

Exp. No.	(a) V_M (mV)	(b) τ_m (μsec)	(c) τ_h	(d) I_{Na} peak (mA/cm^2)	(e) $\bar{g}_{Na}$ (mmho/cm^2)	(f) V_h (mV)	(g) Temp (°C)
790424[a]	−36.0	181	438	0.08	25	− 74	14.5
	−26.5	123	879	0.41			
	−17.0	117	399	1.09			
	− 7.5	77	283	1.40			
	2.0	54	240	1.38			
	11.5	43	199	1.17			
	21.0	35	168	0.90			
	30.5	34	158	0.65			
790426[b]	−36.0	197	1818	1.15	126	− 96	16.0
	− 6.0	69	264	8.23			
	4.0	60	225	6.84			
	14.0	57	193	5.55			
	24.0	53	164	4.05			
	34.0	40	155	2.79			
	44.0	33	117	1.63			
790508 A	−54.0	86	9022	0.31	170	−111	18.1
	−44.5	123	2640	1.18			
	−35.0	165	922	4.27			
	−25.5	125	442	8.33			
	−16.0	95	323	9.60			
	− 6.5	74	253	9.52			
	3.0	63	211	8.69			
	12.5	56	168	7.48			
	22.0	39	162	6.16			
	31.5	40	139	4.70			
790508 B[c]	−27.0	180	1274	1.82	95	− 87	18.1
	−17.0	136	472	4.96			
	− 7.0	86	321	5.83			
	3.0	61	236	5.34			
	13.0	49	193	4.31			
	23.0	43	166	3.31			
	33.0	49	126	2.27			
	43.0	34	106	1.33			

Solution in pools *C* and *E*: CsF-3 at pH = 7.4. Solution in pool *A*: K-free ASW.

Time constants from experiments at temperatures other than 18.1 °C were corrected assuming a Q_{10} of 3.0.

[a] This run was obtained 13 min after switching the solution from K-free ASW plus 500 nM TTX to K-free ASW.

[b] Feedback amplifier in the Dodge-Frankenhaeuser configuration.

[c] Series resistance compensation was used for this run. The holding potential level in column (f) was determined from the measured reversal potential of the sodium currents.

However, later on in this paper we show data suggesting that a holding potential more negative than the resting potential (as for the experiment in Fig. 5) induces a delay both in the start of the activation and in the inactivation of the Na^+ conductance.

τ_h values obtained using the double-pulse protocol (illustrated in Fig. 5) plus τ_h values obtained by fitting a single time constant curve to the inactivating part of g_{Na} enabled us to examine the effects of membrane potential in the range from −80 to 40 mV.

Kinetic and Steady-State Characteristics of the Sodium Conductance

With the cut ends of the fiber in solution CsF-1 (no added Na^+), the $I_{Na}-V$ curve near the reversal potential was always nonlinear (Quinta-Ferreira, 1981) as in the squid giant axon (Keynes & Rojas, 1976). The addition of 47 mM Na^+ (solution CsF-2) transformed the nonlinear $I_{Na}-V$ curve recorded in the absence of internal Na^+ into a linear $I_{Na}-V$ in the potential range from 10 to 80 mV (Quinta-Ferreira, 1981). For this reason, in what follows, we have assumed that the instantaneous current-voltage relations for the sodium system under these experimental conditions is linear. Therefore, to calculate g_{Na} from the I_{Na} records we used

$$g_{Na} = \frac{I_{Na}}{V - V_{Na}}$$

where V_{Na} represents the reversal potential for the inward currents. This was measured from a graph of peak I_{Na} values versus membrane potential.

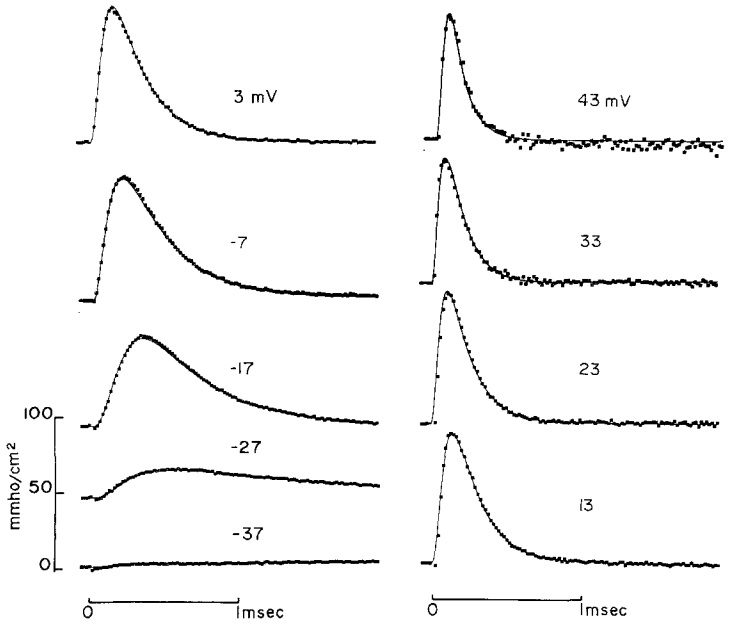

Fig. 6. Time course of g_{Na} as a function of membrane potential during the pulses. Experiment 790508B: Solution in pools *C* and *E* was CsF-3. External solutions: K-free ASW. Feedback amplifier of the Dodge-Frankenhaeuser type. Holding potential set at −87 mV. Fitted curves were calculated with Eq. (2). Interval between points 6 μsec

The $g_{Na}(t)$ curves thus obtained for values of $t > \delta t$ [*see* Eq. (1)] were analyzed assuming the Hodgkin-Huxley formalism (1952*b*). Whence, we may write a single equation with both parts of the conductance as follows

$$g_{Na}(t) = g_{Na,max}(m_\infty - (m_\infty - m_o) \cdot \exp(-(t-\delta t)/\tau_m))^3 \exp(-t/\tau_h) \quad (2)$$

where δt has the same meaning as for Eq. (1). Since in most of our experiments the holding potential was set near −100 mV, m_o could be assumed to be close to zero.

To obtain the various parameters in Eq. (2), $g_{Na}(t)$ records were used to fit a single exponential curve to the points during the falling phase of the conductance. Then the conductance values along the record were divided by $\exp(-t/\tau_h)$ using the time constant τ_h calculated from the first fit. The second step consisted of taking the cubic root of the $g_{Na}(t)/\exp(-t/\tau_h)$ values and conducting a second least-squares fit of a single exponential function to the points. The results of such analysis are illustrated for $9\,g_{Na}(t)$ records in Fig. 6.

τ_m and τ_h values obtained as illustrated in Fig. 6 are presented in Table 3. It should be mentioned here that the method used to fit the $g_{Na}(t)$ curves with Eq. (2) worked quite well provided the potential difference $V - V_{Na}$ in absolute value was greater than 10 mV.

To compare the parameters obtained using this procedure with the values obtained using a computer program designed to minimize residuals, we refitted one record in each experimental series using the method based on Marquardt (1963) and Powell

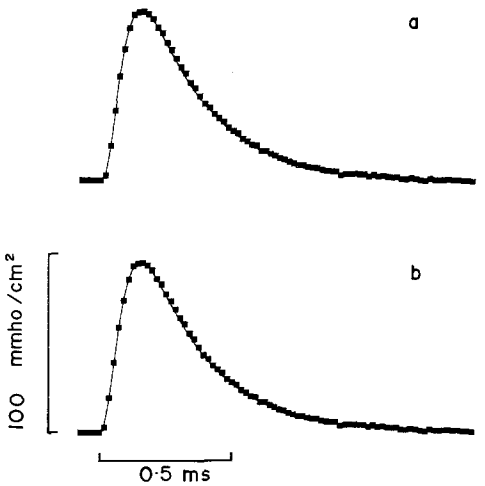

Fig. 7. Least-squares fit of a $g_{Na}(t)$ record using either four or five free parameters. For record in part (*a*): the exponent was fixed at 3.0 and, $\tau_m = 61$ μsec, $\tau_h = 236$ μsec, $\delta t = 37$ μsec and $m_\infty = 0.98$. For record in (*b*) the exponent was 3.3. $\tau_m = 61$ μsec, $\tau_h = 236$ μsec, $\delta t = 33$ μsec, $m_o = 0.0001$ and $m_\infty = 0.98$. Membrane potential during the pulse, 3 mV. For further details, *see* Fig. 6

(1968) in which the following parameters were adjusted to minimize the sum of residuals: τ_m, τ_h, δt, m_∞ and a, the exponent in Eq. (2). For example, consider the records shown in Fig. 7. τ_m and τ_h remained unchanged and δt changed to 37 μsec (from 33 μsec), m_∞ remained unchanged for $a = 3$.

The time constants and the steady-state values provided two relations to calculate the rate constants (Hodgkin & Huxley, 1952*b*). Figure 8 presents the values obtained. The left side of Fig. 8 shows the rate constant values for the *m* process (upper part) and the corresponding time constant (lower part). On the right side, upper part, the rate constant

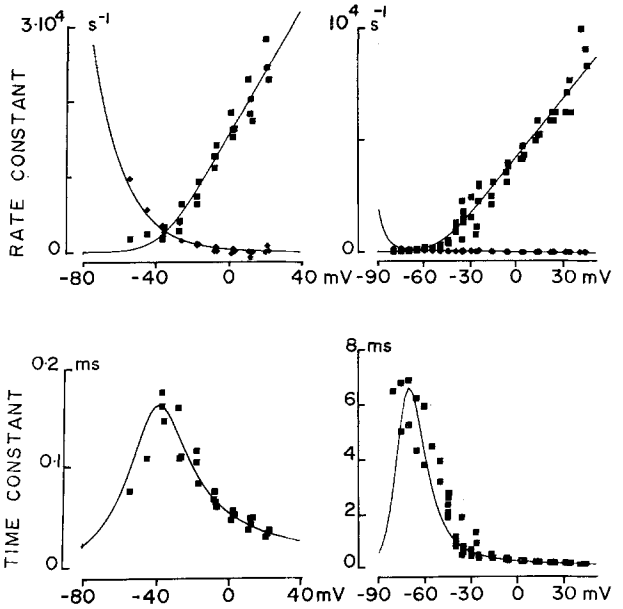

Fig. 8. Rate and time constants for the activation and inactivation of g_{Na}. *Left side, upper part:* ■ $=\alpha_m$; ◆ $=\beta_m$. *Lower part:* τ_m. Rate constants were normalized to 18.1 °C assuming a Q_{10} of 3. Continuous lines represent least-squares regression curves calculated using the following equations:

$$\alpha_m=((A+BV)/(1-\exp(C(A+BV)/B)))10^3,$$

$$\beta_m=(a+bV)(1+\exp(c(d-V)))10^3,$$

$$\tau_m=\frac{1}{\alpha_m+\beta_m},$$ with $A=15.35$, $B=0.42\,\text{mV}^{-1}$, $C=-0.18$, $a=0.15$, $b=-0.003\,\text{mV}^{-1}$, $c=0.05\,\text{mV}^{-1}$, $d=12.0$ mV. *Right side, upper part:* ◆ $=\alpha_h$; ■ $=\beta_h$. *Lower part:* τ_h. Lines were calculated with the following equations:

$$\alpha_h=(A+BV)(1+\exp(C(D-V))),$$

$$\beta_h=(a+bV)/(1-\exp(c(a+bV)/b)),$$

$$\tau_h=\frac{1}{\alpha_h+\beta_h},$$ with $A=12.42$, $B=-0.94\,\text{mV}^{-1}$, $C=0.20\,\text{mV}^{-1}$, $D=-65.0$ mV, $a=4357.2$, $b=87.6\,\text{mV}^{-1}$, $c=-0.18$

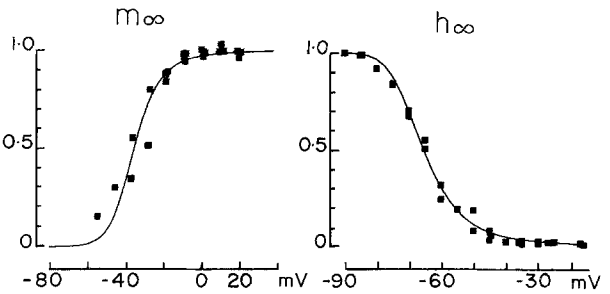

Fig. 9. m_∞-curve (left side) and $h_\infty - V$ curve (right side). For details *see* legend to Fig. 8. Lines were calculated with the following equations:

$$m_\infty=\frac{\alpha_m}{\alpha_m+\beta_m};\quad h_\infty=\frac{\beta_h}{\alpha_h+\beta_h}.$$

Data from same experiments as in Fig. 8

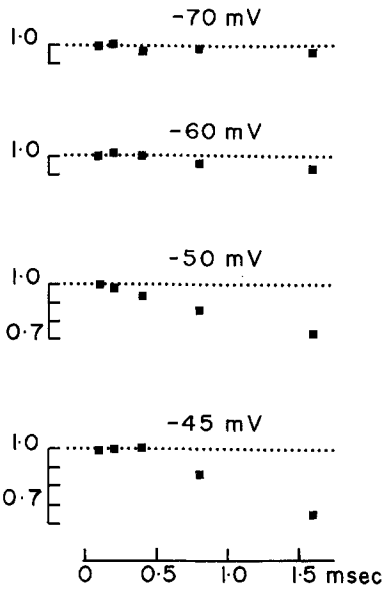

Fig. 10. Initial time course of the development of the fast sodium conductance inactivation. Same experiment as in Fig. 5

values for the h process are plotted and in the lower part the values of the time constant τ_h.

The steady-state values of the variables m and h are plotted as a function of membrane potential in Fig. 9. The curves in Fig. 9 were calculated using the linear-exponential equations which gave the best fit of the experimentally measured rate constants (Woodbury, White, Mackey, Hardy & Chang, 1970). $m_\infty=0.5$ at -35 mV. The slope at this point is $0.04\,\text{mV}^{-1}$ (or 12.5 mV for an e-fold change in m_∞). $h_\infty=0.7$ at -70 mV. The slope at this point is $0.044\,\text{mV}^{-1}$ (or 15.9 mV for an e-fold change in h_∞).

Effects of Hyperpolarization on Sodium Conductance Activation and Inactivation

Resting membrane potential in *Carcinus* fibers in seawater has been estimated as -71 mV (Hodgkin & Huxley, 1945). Using microelectrodes filled with 3 M KCl (50 MΩ tip resistance) we measured values between -69 and -71 mV. The holding potential used during the experiments reported here ranged between -65 and -150 mV. Two results obtained using the double-pulse protocol showed an interesting effect worth presenting and discussing here. First, pulses taking the potential V_1 in the hyperpolarizing direction invariably decreased h_∞. This effect is shown in Fig. 4 where h_∞ decreased from 1.0 at -100 mV to 0.9 measured at -160 mV.

Second, four time courses of the development of the inactivation process from the eight series shown in Fig. 5 have been plotted in Fig. 10 using an expanded time base and show a clear delay in the start of the h process.

The effect of holding potential on the initial delay of the $g_{Na}(t)$ records is presented in Fig. 11 for

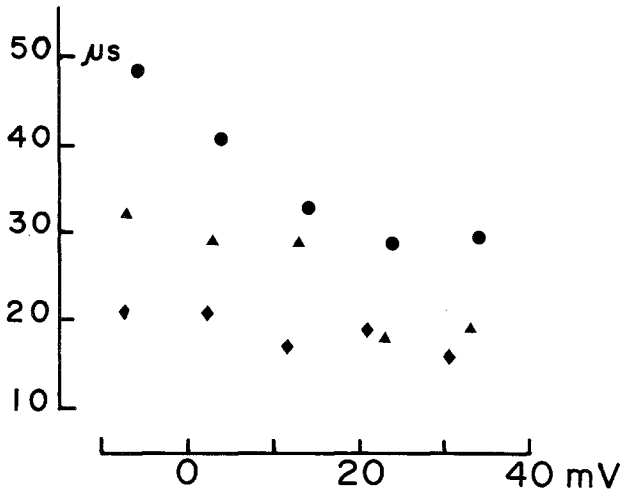

Fig. 11. Effects of membrane potential on δt. Each set of values has been adjusted to 18.1 °C assuming a Q_{10} of 7. The abscissa represents the membrane potential during the depolarizing pulses. ●: Experiment 790426, $V_h = -96$ mV; ▲: Experiment 790508B, $V_h = -87$ mV; ◆: Experiment 790424, $V_h = -74$ mV

three holding potentials. It may be seen that at $V_h = -74$ mV, value close to the true resting potential in these fibers, δt remains almost constant near 20 μsec. At $V_h = -96$ mV, δt decreases from nearly 50 to 30 μsec with the size of the test pulse. These results are very similar to those obtained in the giant axon of the squid (Keynes & Rojas, 1976).

Discussion

The results presented in Figs. 4, 10 and 11 are consistent with the idea that when the membrane is either held at high negative potentials or 20-msec hyperpolarizing pulses are applied a fraction of the Na channels is locked in a closed conformation. A possible explanation for these effects is that the gating structures of the channel undergo a transition from the resting energy state to another requiring more energy to activate. There are several possibilities to explain such a transition (Chapman. 1980), for example, a displacement of the gating structure within the membrane into a region where the fraction of the electric field acting on the gating dipoles is reduced. The net result of such displacement would be a reduction in the valence (effective valence) of the gates (Rojas, 1975).

The initial delay δt in the start of I_{Na} seen in this and in other preparations (Armstrong & Bezanilla, 1974; Keynes & Rojas, 1974, 1976) can be incorporated in the Hodgkin-Huxley equations describing $g_{Na}(t)$, namely,

$$g_{Na}(t) = g_{Na,max}(m_\infty - (m_\infty - m_o) \cdot \exp(-t/\tau_m)^3 \exp(-t/\tau_h) \quad (3)$$

as $\exp(\delta t)$ [Neumcke, Nonner & Stämpfli, 1976; *see* Eq. (2)]. This is required in order to preserve the Hodgkin-Huxley m^3 kinetics, for otherwise a negative value of m_o would be necessary.

The result of a displacement of the gating structure further away from its resting energy state induced by hyperpolarization would be to lock a fraction of the Na channels in a closed state. To activate Na channels in this state the membrane potential during the pulses has to perform work to transfer the gates from this closed state to the resting state (also closed to ion flow) first, and then to transfer the gates to the open state. We propose that this displacement also causes the decrease in h_∞ observed at potentials more negative than −70 mV.

Although proof of this hypothesis cannot be achieved by kinetic analysis, the comparison illustrated in Fig. 7 shows that, with this mechanism, it is possible to preserve the Hodgkin-Huxley formalism and fit the data for the sodium conductance (Armstrong & Bezanilla, 1974; Keynes & Rojas, 1974, 1976); and for the potassium conductance (Cole & Moore, 1960). The development of a kinetic model and the test of the kinetic equations is the subject of another paper (Rojas & Quinta-Ferreira, 1981).

The experimental $g_{Na}(t)$ record was fitted using Eq. (2). The fitting program adjusted the parameters to give the minimum value for the sum of the squares of the residuals (experimental point minus fitted point). For Fig. 7 the exponent in Eq. (2) and m_o were fixed (at 3 and 0, respectively) and for Fig. 7 all the parameters in Eq. (2) were free for adjustment. It may be seen that the experimental curves are well described by Eq. (2).

Comparison of the Kinetic and Steady-State Properties with Other Cells

The results from experiments in which I_{Na} was reduced by treatment with TTX and, after correcting as far as possible from the effects of incomplete compensation for the series resistance, gave $m_\infty - V$ curves with a midpoint at −35 mV. At this point a 12.5-mV change in potential produced an *e*-fold change in m_∞. The midpoint value is almost exactly the same as for the giant axon of squid, namely, −34 mV (Keynes & Rojas, 1976).

Another important parameter to consider is the maximum g_{Na}. The average value from three experiments in Table 3 is 130 mmho/cm^2. This measurement hinges on the accuracy of the estimation of the current calibration factor. This is calculated as (GAIN × AREA × R_{ED}).

All the I_M values in this paper are referred to the membrane area in pool *A* which was estimated from

geometrical measurements. As the separation between the seals in pool A was adjusted to be less than 50 μm, the error in the estimation of the area could be quite large. As in our experiments the ends of the fiber were cut in 500 mM CsF solution, from measurements of the resistivity of the solutions used and assuming the same specific resistance for the axoplasm in contact with this solution, we arrived at a value of 33 Ωcm which was used to calculate R_{ED} from geometrical measurements. Furthermore, in most of the experiments in this paper we have integrated the first 100 μsec of the V_E transient (which is proportional to the membrane current) for 50-mV hyperpolarizing pulses and obtained a specific capacity in the range from 0.7 to 1.1 $\mu F/cm^2$ of membrane in pool A. This last result suggests that the errors introduced in the estimation of the area in pool A and in R_{ED} have cancelled out.

Taking $g_{Na,max}$ as 130 mmho/cm^2 and the conductance of a single Na channel estimated in the squid axon as 5×10^{-12} mho (Rojas, 1973) one obtains

$$A = g_{Na,max}/\gamma_{Na} = 260\ \mu m^{-2}.$$

This density is 5.3 times larger than the value estimated for nerves from the walking leg of the crab *Maia squinado* measuring TTX binding (Keynes et al., 1971). While the |TTX| at which the amplitude of the compound action potential is reduced to half is about 14 nM in *Maia* nerves, the |TTX| at which g_{Na} is reduced to half is about 5 nM in *Carcinus axons.*

There are two possible explanations for these differences. It is known from TTX binding studies that the Na channel density is a function of the diameter of the nerve fibers. As with the measurements of the compound action potential one is testing fibers with different diameters (Abbot, Hill & Howarth, 1958) it is possible that the large proportion of fibers with diameters smaller than 15 μm in *Maia* nerves may be the cause as the density decreases to a few Na channels/μm^2 in small fibers (Ritchie, Rogart & Strichartz, 1976). As for the difference in the |TTX| required to obtain 50% blockage the explanation could be either a difference in the affinity of the sodium sites for TTX in the different fibers, or that the relationship between g_{Na} and size of the compound action potential is nonlinear, or both.

In general, the voltage dependence of τ_m and τ_h are as described by Hodgkin and Huxley (1952*b*). If we allow for a temperature correction, assuming a Q_{10} of 3, the maximum τ_m value in Table 3 at 6 °C would be 648 μsec while for the squid giant axon is little over 500 μsec (Keynes & Rojas, 1976).

This research was supported by the Science Research Council. It was submitted by E. Quinta-Ferreira as part of a Ph.D. thesis for the School of Biological Sciences, University of East Anglia. During this work E. Quinta-Ferreira was supported by the Calouste Gulbenkian Foundation. The secretarial assistance of Mrs S. Garrod is acknowledged.

References

Abbot, B.C., Hill, A.V., Howarth, J.V. 1958. The positive and negative heat production associated with a single impulse. *Proc. R. Soc. London B* **148**:149–187

Arispe, N., Quinta-Ferreira, E., Rojas, E. 1979. Gating of the sodium conductance in the giant axon of the crab *Carcinus maenas*. *J. Physiol. (London)* **295**:11P–12P

Armstrong, C.M., Bezanilla, F. 1974. Charge movement associated with the opening and closing of the activation gates of the Na-channels. *J. Gen. Physiol.* **63**:533–552

Chapman, J.B. 1980. Consistency between thermodynamics and the kinetics of m, n and h in the Hodgkin-Huxley equations. *J. Theor. Biol.* **85**:487–495

Cole, K.S., Hodgkin, A.L. 1939. Membrane and protoplasm resistance in the squid giant axon. *J. Gen. Physiol.* **22**:671–687

Cole, K.S., Moore, J. 1960. Ionic current measurements in the squid giant axon membrane. *J. Gen. Physiol.* **44**:123–167

Connor, J.A. 1975. Neural repetitive firing: A comparative study of membrane properties of crustacean walking leg axons. *J. Neurophysiol.* **38**:922–932

Connor, J.A., Walter, D., McKown, R. 1977. Neural repetitive firing. Modifications of the Hodgkin-Huxley axon suggested by experimental results from crustacean axons. *Biophys. J.* **18**:81–102

Dodge, F.A., Frankenhaeuser, B. 1958. Membrane currents in isolated frog nerve fiber under voltage clamp conditions. *J. Physiol. (London)* **143**:76–90

Frankenhaeuser, B., Lindley, B.D., Smith, R.S. 1966. Potentiometric measurement of membrane action potentials in frog muscle fibers. *J. Physiol. (London)* **183**:152–166

Goldman, D.E. 1943. Potential, impedance and rectification in membranes. *J. Gen. Physiol.* **27**:37–60

Hille, B., Campbell, D.T. 1976. An improved Vaseline gap voltage clamp for skeletal muscle fibers. *J. Gen. Physiol.* **67**:265–293

Hodgkin, A.L., Huxley, A.F. 1945. Resting and action potentials in single nerve fibres. *J. Physiol. (London)* **104**:176–195

Hodgkin, A.L., Huxley, A.F. 1952*a*. The dual effect of membrane potential on sodium conductance in the giant axon of *Loligo*. *J. Physiol. (London)* **116**:497–506

Hodgkin, A.L., Huxley, A.F. 1952*b*. A quantitative description of membrane current and its application to conduction and excitation in nerve. *J. Physiol. (London)* **117**:500–544

Hodgkin, A.L., Katz, B. 1949. The effect of sodium ion on the electrical activity of the giant axon of the squid. *J. Physiol. (London)* **108**:37–77

Keynes, R.D., Ritchie, J.M., Rojas, E. 1971. The binding of tetrodotoxin to nerve membranes. *J. Physiol. (London)* **213**:235–254

Keynes, R.D., Rojas, E. 1974. Kinetics and steady-state properties of the charged system controlling sodium conductance in the squid giant axon. *J. Physiol. (London)* **239**:393–434

Keynes, R.D., Rojas, E. 1976. The temporal and steady-state relationships between activation of the sodium conductance and movement of the gating particles in the squid giant axon. *J. Physiol. (London)* **255**:157–189

Marquardt, D.W. 1963. An algorithm for least-squares estimation of non-linear parameters. *J. Soc. Ind. Appl. Math.* **11**:431–441

Moore, J.W., Narahashi, T., Shaw, T.I. 1967. An upper limit to the number of sodium channels in nerve membrane? *J. Physiol. (London)* **188**:99–105

Neumcke, B., Nonner, W., Stämpfli, R. 1976. Asymmetrical displacement current and its relation with the activation of sodium current in the membrane of frog myelinated nerve. *Pfluegers Arch.* **363**:193–203

Nonner, W. 1969. A new voltage clamp method for Ranvier nodes. *Pfluegers Arch.* **309**:176–192

Powell, M.J.D. 1968. A FORTRAN subroutine for solving systems of non-linear algebraic equations. Harwell Report AE-RE-R 5947, H.M. Stationery Office

Pynsent, R.B., Rojas, E. 1979. Voltage clamp and data acquisition method for single myelinated nerve fibre work. *J. Physiol. (London)* **291**:14P–15P

Quinta-Ferreira, M.E. 1981. Ionic channels in the giant axon of the crab *Carcinus maenas*. Ph.D. Thesis. School of Biological Sciences, University of East Anglia, Norwich

Ritchie, J.M., Rogart, R.B., Strichartz, G.R. 1976. A new method for labelling saxitoxin and its binding to non-myelinated fibres of the rabbit vagus, lobster walking leg, and garfish olfactory nerves. *J. Physiol. (London)* **261**:477–494

Rojas, E. 1973. The conductance of a single sodium channel in squid giant axons from *Loligo*. *Acta Physiol. Lat. Am.* **23**:90–92

Rojas, E. 1975. Gating mechanism for the activation of the sodium conductance in nerve membranes. *Cold Spring Harbor Symp. Quant. Biol.* **XL**:305–320

Rojas, E., Quinta-Ferreira, E. 1981. Sodium channel gating in excitable membranes. Proceedings VII International Biophysics Congress and the III Pan American Biochemistry Congress, Mexico City, Mexico

Woodbury, J.W., White, S.H., Mackey, M.C., Hardy, W.L., Chang, D.B. 1970. Biochemistry. University of Washington Press, Seattle

Received 5 March 1981; revised 10 July, 23 October 1981